International Journal of Heat and Mass Transfer 115 (2017) 871–881

Contents lists available at ScienceDirect

International Journal of Heat and Mass Transfer

journal homepage: www.elsevier.com/locate/ijhmt

Sobol sensitivity analysis for governing variables in design of a plate-fin heat exchanger with serrated fins

Huizhu Yang [a,d], Jian Wen [a], Simin Wang [b,*], Yanzhong Li [a], Jiyuan Tu [c], Wenjian Cai [d]

[a] Department of Refrigertation and Cryogenics Engineering, School of Energy and Power Engineering, Xi'an Jiaotong University, Xi'an 710049, China
[b] Department of Process Equipment and Control Engineering, School of Chemical Engineering and Technology, Xi'an Jiaotong University, Xi'an 710049, China
[c] Institute of Nuclear and New Energy Technology, School of Materials Science and Engineering, Tsinghua University, Beijing 100084, China
[d] EXQUISITUS, Centre for E-City, School of Electrical and Electronic Engineering, Nanyang Technological University, Singapore 639798, Singapore

ARTICLE INFO

Article history:
Received 30 May 2017
Received in revised form 21 August 2017
Accepted 26 August 2017

Keywords:
Plate-fin heat exchanger
Sensitivity analysis
Design optimization
Sobol method
Serrated fin

ABSTRACT

Sobol sensitivity analysis can quantify the impact of input parameters' variations on the performance of plate-fin heat exchanger to guide the selection of input variables during design procedure. In this paper, the Reynolds number *Re*, fin height *h*, fin space *s*, fin thickness *t* and interrupted length *l* are considered as five input parameters, while exchanger volume, exchanger material content, heat flow rate and pressure drop with different constraints are taken as the design objectives. Moreover, to study the impact of Prandtl number on input parameters, the Sobol sensitivity indices of five parameters are compared for air and water. The results show that the Reynolds number *Re* and fin space *s* are the two main factors that affect the performance of plate fin heat exchanger. As the heat exchanger size limited, a smaller fin thickness *t* is selectable. Compared with air, the interrupted length *l* should be selected a smaller value for water. Guidance about the fin surface selection is given. Sobol sensitivity analysis methods can be performed to detect the importance of parameters in various complex engineering applications. And compared with other optimization algorithms, this method is simple to implement.

1. Introduction

When the duty requirement (inlet and outlet temperatures and fluid flow rates) and the pressure drop are given, the typical steps for plate-fin heat exchanger (PFHE) thermohydraulic design include the selection of fin type, flow arrangement, the determination of fin configuration, fluid operating that involves the determination of *Re*, the *j* and *f* data acquisition, if any, layer pattern optimization. The exchanger fin type and flow arrangement are firstly selected based on the problem specification and experience. For a PFHE, Hesselgreaves [1] proposed that if heat capacity rate ratio $C^* > 0.25$ ($C^* = C_{min}/C_{max}$), and especially if the required effectiveness $\varepsilon > 0.8$, a counterflow configuration is the most economic design; If $C^* < 0.25$, the flow arrangement configuration makes little difference to the effectiveness, a crossflow design is most appropriate because of its simplicity. The fin surface selection that involves the definition of the fin height *h*, fin thickness *t*, fin space *s*, interrupted length *l* and so on. Under different constrained conditions, the fin surface of PFHEs had been optimized by using different strategies based on genetic algorithm [2–6], imperialist competitive algorithm [7], particle swarm optimization algorithm [8–10], hybrid evolutionary algorithm [11,12] and learning automata based particle swarm optimization [13] for various objectives, such as minimization of total weight, minimization of total annual cost, entropy generation minimization, minimum pressure drop, maximum effectiveness and maximum heat flow rate. However, when it comes to the actual design, the optimized parameters of fin surface to be employed on PFHE design will be a problem because those studies generally apply in specific conditions. Besides, it is difficult for designers to apply those methods to help themselves to select the most beneficial fin surface among the various fin surfaces due to the complexity of those methods application procedures. Therefore, until now, the fin surface is determined mainly based on the empirical chosen but lack the theoretical guidance.

The channel *Re* is closely associated with many factors, such as the pressure drop, heat flow rate, the ratio *j*/*f*, surface efficiency, number of thermal units and hydraulic diameter. That will describe in detail below. The Colburn heat transfer factor *j* and Fanning friction factor *f* were often calculated using the empirical equations. When the air was used as the working media, Kays and London [14], Manson [15], Joshi and Webb [16], Wieting [17], Mochizuki et al. [18], Dubrowsky [19], Manglik and Bergles

* Corresponding author.
E-mail address: smwang@mail.xjtu.edu.cn (S. Wang).

http://dx.doi.org/10.1016/j.ijheatmasstransfer.2017.08.089
0017-9310/

Nomenclature

Latin symbols

α	heat transfer coefficient, W m^{-2} K^{-1}
A	heat transfer area, m^2
A_c	flow area, m^2
c_p	specific heat, J kg^{-1} K^{-1}
D	hydraulic diameter of fin channel, m
$D_i(Y)$	first-order variance
$D_{ij}(Y)$	two-order interaction
$D_{ij\cdots k}(Y)$	high-order interaction
f	friction factor
G	mass velocity, kg m^{-2} s^{-1}
h	fin height, m
j	Colburn factor
l	interrupted length, m
L	length, m
m	mass flow rate
N	number
Nu	Nussle number
NTU	number of thermal unit
Δp	pressure drop, Pa
Pr	Prandtl number
Q	total rate of heat transfer, W
Re	Reynolds number
s	fin space, m
S_i	first-order sensitivity index
S_{ij}	two-order sensitivity index
$S_{ij\cdots k}(Y)$	high-order sensitivity index
S_{Ti}	total sensitivity index
T	temperature, K
t	fin thickness, m
u	velocity, m s^{-1}
U	total heat transfer coefficient, W m^{-2} K^{-1}
V	volume, m^3
V_m	material content, kg
Var(Y)	total variance of the output goals
X	parameters
Y	target function

Greek symbols

δ	thickness of cover plate, m
ρ	density, kg m^{-3}
μ	viscosity, kg m^{-1} s^{-1}
λ	thermal conductivity, W m^{-1} K^{-1}
ε	effectiveness
η	efficiency
σ	porous ratio

Subscripts

c	cold side
h	hot side
H	height
i	inlet
L	length
o	outlet
w	wall
W	width

[20] and Yang and Li [21] had provided different empirical correlations for PFHEs with serrated fins based on experimental data or based on numerically investigated by Kim and Lee [22]. But, for high Prandtl fluid, using those empirical equations to calculate the j and f factors might produce large errors because those empirical equations are generally greatly affected by the type of working media. According to the research of Hu and Herold [23], for water and ethylene glycol, the value of the experimental j factor was approximately twice as big as the value of the empirical equation. Unfortunately, there is scarce data for the high Prandtl fluid. Finally, layer pattern optimization is needless or eases when the heat transfer occurs among few fluids.

Sensitivity analysis is capable to quantify the relative importance of design parameters in determining the value of an assigned output objective function. Thus, the most influential parameters and weak impact parameters from a set of parameters can be determined by using the sensitivity analysis. The sensitivity analysis method mainly includes differential method, regression method, screen method, variance based method and so on. The differential method only explores a reduced space of the input factor around a base case, and the regression method is only suitable for linear models or monotonic functions. The screen method only provide qualitative the effects of different factors on outputs. Compared with the above-mentioned methods, the variance based method can quantify the effects of different factors, confirms the interactions between factors and is suitable for nonlinear and non-additive models, etc. The drawback of this approach is its high computational expensive. More detailed information about the advantages and disadvantages of these methods can be found in the literature [24]. Lerou et al. [25] and Wen et al. [26] optimized the geometry of PFHEs using one-factor-at-a-time methods. Kotcioglu et al. [27] reported optimum values of design parameters in a heat exchanger with a rectangular duct by Taguchi method. Fesanghary et al. [28] explored the use of global sensitivity analysis and harmony search algorithm for design optimization of shell and tube heat exchangers. Qi et al. [29] studied five experimental factors affecting the heat transfer and pressure drop of a heat exchanger with corrugated louvered fins using the Taguchi method. Detecting effects of design parameters can greatly reduce parameter uncertainties and increase the model accuracy. In practice, sensitivity analysis is very suitable for engineering applications because it is characterized by simple to implement, easy to interpret and low computational cost. However, few researches about the sensitivity analysis of PFHE with serrated fin have been published.

The aim of the present paper is to quantitatively evaluate the effects of different parameters to guide the design of PFHE with serrated fins. Therefore, Sobol sensitivity analysis was applied to study the effects of Re, fin height h, fin space s, fin thickness t and interrupted length l on the performance of PFHE. Besides, in order to study the Prandtl number effect, the effects of different parameters on the objective functions were studied for air and water as the working media, separately.

2. Design methodology and Sobol method

2.1. Thermohydraulic model

In this section, the equations for calculating heat exchanger volume and material content are presented for fixed heat flow rate and pressure drop in a counter flow PFHE. Moreover, the equations of the heat flow rate and pressure drop are also shown for fixed heat exchanger size. To better study the sensitivity of different parameters on the objective functions, the configuration parame-

ters of serrated fin and mass flow rate in both hot and cold sides are identical and the heat transfer occurs in two fluids. The schematic diagram of the fin surface and the heat exchanger core are shown in Fig. 1.

2.1.1. Fixed heat flow rate and pressure drop

When the mass flow rate m is fixed and a flow balance, characterized by m_h=m_c, the effectiveness ε is defined as:

$$\varepsilon = \frac{T_{h,i} - T_{h,o}}{T_{h,i} - T_{c,i}} \tag{1}$$

where T is temperature. The subscript i, o, h and c are inlet, outlet, hot side and cold side, respectively.

For counter flow, the number of thermal unit for one side ntu is calculated as:

$$ntu = NTU = \frac{\varepsilon}{1-\varepsilon} \tag{2}$$

The mass velocity G is defined as:

$$\Delta p = \frac{1}{2}\rho u^2 \frac{4L_L}{D} f = \frac{G^2}{2\rho}\frac{4L_L}{D} f \tag{3}$$

$$G = \sqrt{\frac{2\rho\Delta p}{f}\frac{D}{4L_L}} \tag{4}$$

where ρ is density. Δp is the allowable pressure drop for one side. u is the velocity. D is hydraulic dimeter. L_L is the flow length of heat exchanger. And the $D/4L_L$ is derived as:

$$D = \frac{4A_c}{A} L_L \tag{5}$$

$$\frac{D}{4L_L} = \frac{A_c}{A} \tag{6}$$

where A_c is the flow area. A is the heat transfer area. And the A_c/A is derived as:

$$Q = \alpha A \Delta t_w = m_h c_{p,h}(T_{h,i} - T_{h,o}) \tag{7}$$

$$j = \frac{Nu}{RePr^{1/3}} = \frac{\alpha D}{\lambda}\frac{A_c\mu}{mD}\frac{1}{Pr^{1/3}} \tag{8}$$

$$\alpha = \frac{jmc_p}{A_c Pr^{2/3}} \tag{9}$$

$$ntu = \frac{\eta_o \alpha A}{mc_p} = \frac{\eta_o Q}{\Delta t_w mc_p} = \eta_o \frac{T_{h,i} - T_{h,o}}{\Delta t_w} \tag{10}$$

$$\frac{A_c}{A} = \frac{\eta_o j}{ntu Pr^{2/3}} \tag{11}$$

where α is heat transfer coefficient. μ is viscosity. λ is the thermal conductivity. Nu is Nussle number. Pr is Prandtl number. η_o is overall efficiency. The subscript w is the wall surface.

Therefore, the mass velocity G is obtained as:

$$G = \sqrt{\frac{2\eta_o\rho\Delta p}{Pr^{2/3} ntu}\frac{j}{f}} \tag{12}$$

where the fin efficiency and overall efficiency are calculated as:

$$\eta_f = \frac{\tanh MH}{MH} \tag{13}$$

$$\eta_0 = 1 - (1-\eta_f)\frac{A_f}{A_f + A_p} \tag{14}$$

where $M = \left(\frac{2\alpha}{\lambda_w t}\right)^{0.5}$. $H = h/2$. A_p and A_f are the primary surface and secondary surface of fin, respectively.

And for air, the j and f factors are obtained by the correlations of Mangles & Bergles [20] or it is obtained by CFD simulation for water.

$$j = 0.6522 Re^{-0.5403}\alpha^{-0.1541}\delta^{0.1499}\gamma^{-0.0678} \times [1 + 5.269\times 10^{-5} Re^{1.34}\alpha^{0.504}\delta^{0.456}\gamma^{-1.055}]^{0.1} \tag{15}$$

$$f = 9.6243 Re^{-0.7422}\alpha^{-0.1856}\delta^{0.3053}\gamma^{-0.2659} \times [1 + 7.669\times 10^{-8} Re^{4.429}\alpha^{0.92}\delta^{3.767}\gamma^{0.236}]^{0.1} \tag{16}$$

where $\alpha = \frac{s-t}{h-t}$, $\delta = \frac{t}{l}$, $\gamma = \frac{t}{s-t}$, and the Re and hydraulic diameter D are calculated as:

$$Re = \frac{GD}{\mu} \tag{17}$$

$$D = \frac{4l(h-t)(s-t)}{2(l(h-t) + l(s-t) + t(h-t)) + t(s-t)} \tag{18}$$

Thus, the flow length L_L and flow area A_c are obtained as:

$$L_L = \frac{\rho D\Delta p}{2G^2 f} \tag{19}$$

$$A_c = \frac{m}{G} \tag{20}$$

Adjusting the layer number of channels N_H and the channel number in each layer N_W, the width L_W and height L_H of heat exchanger are obtained as:

$$A_c = N_W N_H (s-t)(h-t) \tag{21}$$

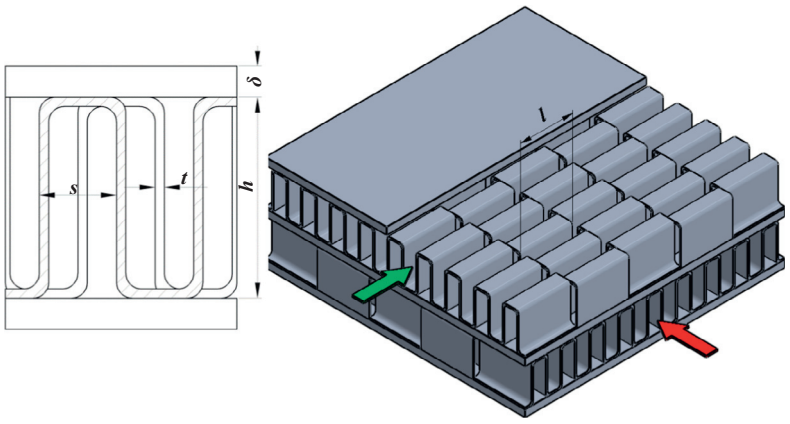

Fig. 1. The schematic diagram of heat exchanger.

$$L_W = N_W s \tag{22}$$

$$L_H = N_H(h+\delta)+\delta \tag{23}$$

After that the flow area A_c and mass velocity G are recalculated. If deviations between the latest two mass velocities are less than 1×10^{-6}. The heat exchanger volume and material content are obtained by Eqs. (24) and (25). If not, re-establish the mass flow rate and return to the above calculate.

The heat exchanger volume is given by:

$$V = L_W L_H L_L \tag{24}$$

And the heat exchanger material content is given by:

$$V_m = V(1-\sigma) \tag{25}$$

where $\sigma = \frac{(s-t)(h-t)}{s(h+\delta)}$ is the porous ratio.

When the Re is given, the data of j and f factor, heat transfer coefficient α, mass velocity G and flow length L_L of heat exchanger are obtained by the above Eqs. (15), (16), (8), (17) and (19).

Here, set a value for mass flow rate m_s. Therefore, the outlet temperature of hot fluid is defined as:

$$T_{h,o} = T_{h,i} - \frac{Q}{m_s c_p} \tag{26}$$

For counter flow and flow balance, the logarithmic mean temperature difference Δt is calculated as:

$$\Delta t = T_{h,o} - T_{c,i} \tag{27}$$

And the heat flow rate Q is defined as:

$$Q = UA\Delta t \tag{28}$$

When the wall thermal resistance is neglected, the overall heat transfer coefficient U and heat transfer areas A are calculated as:

$$U = \frac{\alpha}{2} \tag{29}$$

$$A = N_B N_H \frac{L_L}{l}[2l(h+s-2t)+2t(s-t)+t(s-2t)] \tag{30}$$

Therefore, based the above equations, the layer number of channels N_H and the channel number in each layer N_W can be obtained, after that the flow area A_c and mass flow rate m are calculated as:

$$A_c = N_W N_H (s-t)(h-t) \tag{31}$$

$$m = GA_c \tag{32}$$

If $|m-m_s| \leqslant 1\times10^{-6}$, the heat exchanger volume and material content are obtained by Eqs. (24) and (25). If not, re-establish the mass flow rate and return to calculate.

Besides, for counter flow and flow balance, the effectiveness ε that considers the wall conduction effect is studied as below:

$$1-\varepsilon = \frac{1}{1+\gamma NTU} \tag{33}$$

$$\gamma = \frac{1+P_\lambda[P_\lambda NTU/(1+P_\lambda NTU)]^{1/2}}{1+P_\lambda NTU} \tag{34}$$

$$P_\lambda = \frac{\lambda_w A_w/L_L}{mc_p} \tag{35}$$

2.1.2. Fixed heat exchanger size and Re

As the width L_W, height L_H and flow length L_L of heat exchanger and Re are given, the flow area A_c, mass flow rate m and heat transfer coefficient α are obtained by Eqs. (21), (20) and (8).

And the heat transfer A is defined as:

$$A = \frac{L_H-\delta}{(h+\delta)}\frac{L_W}{s}\frac{L_L}{l}(2l(h+s-2t)+2t(s-t)+t(s-2t)) \tag{36}$$

Therefore, the pressure drop of heat exchanger is obtained by Eq. (3).

The number of thermal unit NTU is calculated as:

$$NTU = ntu = \frac{(\eta_o \alpha A)}{mc_p} \tag{37}$$

As a consequence, the effectiveness ε is obtained by Eq. (2), and the outlet temperature $T_{h,o}$ of hot fluid and the heat flow rate are calculated as:

$$T_{h,o} = T_{h,i} - (T_{h,i} - T_{h,o})\varepsilon \tag{38}$$

$$Q = mc_p(T_{h,i} - T_{h,o}) \tag{39}$$

2.2. Sobol method

The effect of input parameters on PFHE performance is complicated. In this study, Sobol method is applied to survey the sensitivity of input parameters because it can quantify the effects of input parameters on output goals and is suitable to handle the complex nonlinear models, non-monotonic models and models with interaction among parameters. Besides, to cover the design range of majority of serrated fin, Re varies from 200 to 2000, fin height h is 3–12 mm, fin space s is 1.4–4.2 mm, fin thickness t is 0.1–0.5 mm and interrupted length l is 3–9 mm.

Based on the variance decomposition, the attribution of total output variance to input parameters and their interactions can be written as follow:

$$Var(Y) = \sum_{i=1}^{d} D_i(Y) + \sum_{i<j}^{d} D_{ij}(Y) + \cdots + D_{12\cdots d}(Y) \tag{40}$$

where Var(Y) is the total variance of the output goals; $D_i(Y)$ is the first-order variance for each parameter X_i and $D_{ij}(Y)$ is the two-order interaction between X_i and X_j. And the calculation of them is defined as:

$$Var(Y) = E(Y_i^2) - E^2(Y_i) \tag{41}$$

$$D_i(Y) = Var[E(Y|X_i)] = \sum_{i=1}^{n} E^2(Y|x_i=\tilde{x}_i)p_i(\tilde{x}_i) - E^2(Y) \tag{42}$$

$$D_{ij} = Var[E(Y|X_i,X_j)] - D_i(Y) - D_j(Y) \tag{43}$$

$$D_{ij\cdots k} = Var[E(Y|X_i,X_j,\cdots,X_k)] - \sum_{k-1} D_{ij\cdots(k-1)} \tag{44}$$

Thus, the first-order sensitivity indexes S_i, the two-order sensitivity indexes S_{ij}, the high-order sensitivity indexes $S_{ij\cdots k}$ and the total-order sensitivity indexes S_{Ti} are written as follow:

$$S_i = \frac{D_i(Y)}{Var(Y)} \tag{45}$$

$$S_{ij} = \frac{D_{ij}(Y)}{Var(Y)} \tag{46}$$

$$S_{ij\cdots k} = \frac{D_{ij\cdots k}}{Var(Y)} \tag{47}$$

$$S_{Ti} = S_i + \sum_{j\neq i} S_{ij} + \cdots + \sum_{j\neq i,k\neq i,j<k} S_{ij\cdots k} \tag{48}$$

The difference between the first-order sensitivity index and the total-order sensitivity index can be regarded as a measure for the interactions between parameter X_i and the other parameters. Besides, as a simplified calculation, the total-order sensitivity index S_{Ti} is obtained as:

$$S_{Ti} = 1 - \frac{D_{-i}(Y)}{Var(Y)} \tag{49}$$

$$D_{-i}(Y) = Var[E(Y|X_{-i})] \tag{50}$$

where X_{-i} is indicated as the variation of all parameters, except X_i.

3. Numerical model

3.1. Physical model

Fig. 2 shows the schematic diagram of a 3D computational domain for CFD simulation, in which only two fin channels perpendicular to the flow direction are studied because of the periodic characteristics. Besides, the entrance part and exit part are considered here in order to make the simulation process close to the actual experimental test and eliminate the influence of reflux.

3.2. Numerical method and meshing

The shear-stress transport (SST) k-ω model developed by Menter [30] is adopted in the simulation, which effectively blends the robust and accurate formulation of the k-ω model in the near-wall region and the freestream independence of the k-ε model in the far field. The governing equation that describes the fluid flow and heat transfer can be defined by using a uniform control equation:

$$\frac{\partial(\rho\phi)}{\partial t} + div(\rho u\phi) = div(\Gamma grad\phi) + S \tag{51}$$

where ϕ is a generalized variable that represents the component velocity u, v, w, the temperature T, the turbulence kinetic energy k, and the turbulence kinetic energy dissipation rate ε. Γ is the generalized diffusion coefficient and S is the generalized source.

Boundary conditions are as follows: the mass flow inlet condition with an inlet temperature of 300 K is carried out in the flow inlet and the pressure drop outlet is set in the flow outlet; the surfaces of the upper and lower cover plate are modeled with a constant temperature of 373.15 K; the periodic boundary conditions are applied on the two sides because of the periodic characteristic of the fins; and non-slip and coupled thermal boundary condition are adopted at the interface between the fluid and solid. The material of heat exchange is aluminum and water is adopted as working fluid where its properties are assumed to be constant. Besides, heat loss is neglected.

The computational domain is meshed with hexahedral grids using ansys meshing, in which a grid refinement is generated at the near-wall region for more precisely determining the turbulent effects. Besides, the grid independence test is carried out by adopting different grid distributions, in which the non-dimensional distance y^+between the first interior node and solid wall is selected 1, 1.3, 1.6 and 2, respectively, as shown in Table 1. It was found that the deviations of the j and f factors for the last three models are less than 1%. Therefore, the grid numbers 5,989,104 can ensure a satisfactory solution in this case. The grid production method is applied to guarantee the non-dimensional distance $y^+ \leq 1.6$ in this study. Besides, for the numerical calculation, the governing equations are iteratively solved by the finite-volume-method with SIMPLE pressure-velocity coupling algorithm and discretized by the second-order upwind scheme. The convergence criterion is that the normalized residuals are less than 1×10^{-6} for the flow equations and 1×10^{-8} for the energy equation. The parallel computations with 8 numbers of processes are performed with a workstation that its CPU frequency is 4 GHz, and it usually takes approximately 8 h for each task.

3.3. Model validation

For model validation, numerical results are compared with the experimental data of the plate 3 from Hu and Herold [23], in which the results obtained by the SST k-ω and those by the low-Re k-ε are also compared. As shown in Fig. 3, the variation trend of j factor and f factor with Reynolds number is in a good agreement with the experimental data. In the j factor values, the RMS values of the percent differences are 10.1% for those of SST k-ω model and 22.4% for those of low-Re k-ε model. While the RMS values of the percent differences in the f values are 14.9% for those of SST k-ω

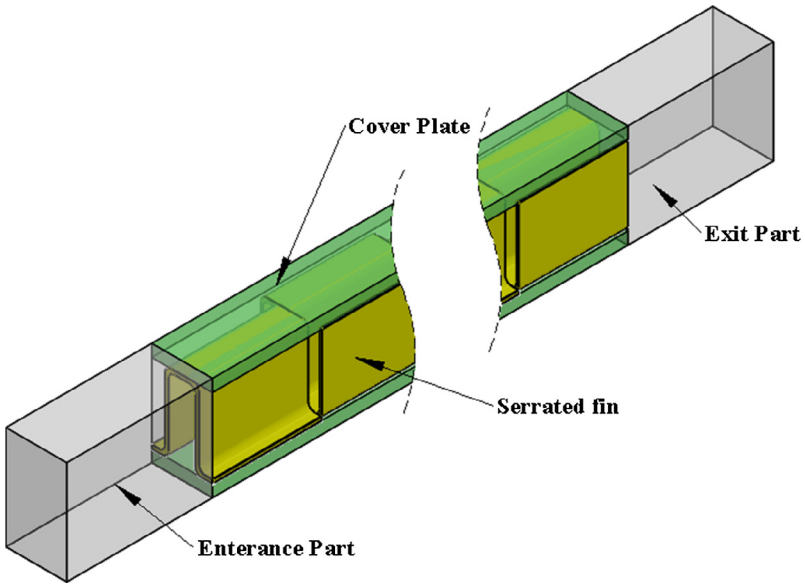

Fig. 2. The computational domain for serrated fin model.

Table 1
Grid independence test.

Grid number	Colburn factor *j*	Friction factor *f*
4,647,042	0.00707	0.0535
5,989,104	0.00709	0.05319
8,953,562	0.00713	0.05294
11,628,691	0.00714	0.05276

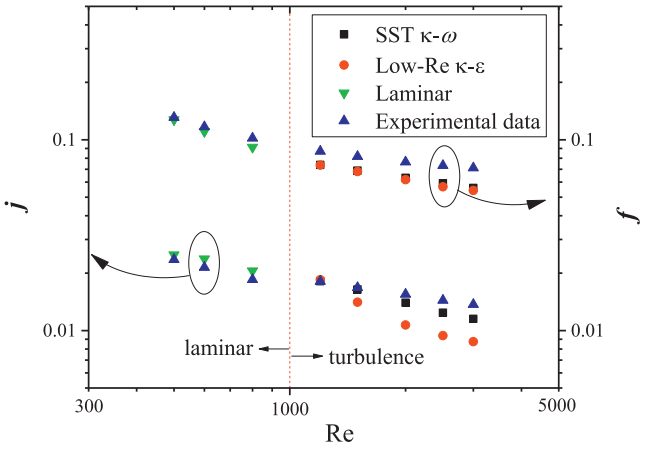

Fig. 3. Comparison of the numerical values and the experimental data.

model and 16.2% for those of low-*Re* *k*-ε model. Therefore, it can demonstrate that the present simulation model is satisfactorily accurate to calculate the *j* and *f* factors for serrated fins when the SST *k*-ω model is adopted to study the turbulent effects. Here, SST *k*-ω turbulent model is used in the region of *Re* > 1000.

4. Results and discussions

In this study, the Sobol sensitivity indices of design parameters are computed by the three-level full factorial designs that includes 243 ($N = 3^5$) design points.

4.1. The effects of parameters for air

4.1.1. Fixed mass flow rate, heat flow rate and pressure drop

The Sobol sensitivity indices of fin height *h*, fin space *s*, fin thickness *t* and interrupted length *l* on heat exchanger volume and material content are presented in Figs. 4 and 5 for fixed mass flow rate, heat flow rate and pressure drop. From the Fig. 4, it can be clearly observed that the fin space *s* is the most important parameter, while the effects of other parameters are low, especially the fin height *h* and interrupted length *l*. The first order sensitivity indices of fin height *h*, fin space *s*, fin thickness *t* and interrupted length *l* are 4.67%, 85.77%, 0.62% and 1.99%, respectively. And the sums of first order sensitivity indices and total-order sensitivity indices are 93.1% and 107.6%, respectively. In Fig. 5, the fin space *s* is also the most important parameter, the effects of the fin height *h* and fin thickness *t* are second-class and the effect of interrupted length *l* is the lowest. Moreover, the sums of first order sensitivity indices and total-order sensitivity indices are 95.3% and 105.2%, respectively. Considering the difference between the first order sensitivity index and total-order sensitivity index can show the effects of interactions among parameters since the total-order sensitivity index includes both first order and higher-order effects. Therefore, it can be inferred, when the mass flow rate, heat flow rate and pressure drop are fixed, the effects of interactions among four parameters on the exchanger volume and material content are low and can be ignored. Moreover, the fin space *s* has the most important effect, while the interrupted length *l* can fix for its effect is tiny on the exchanger volume and material content.

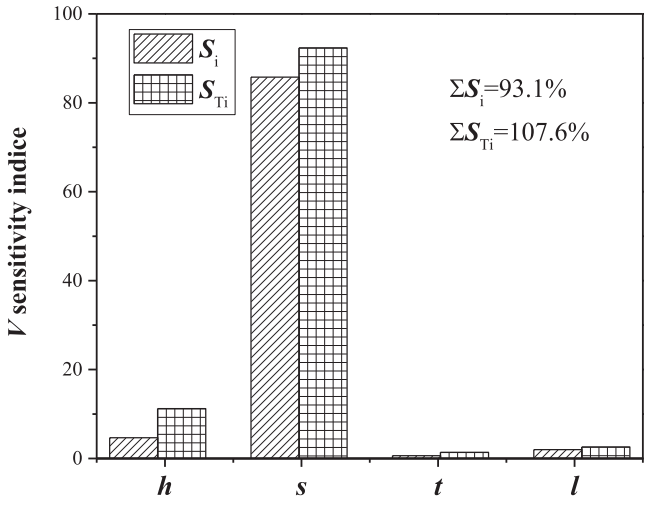

Fig. 4. Evolution of effect of parameters of *h*, *s*, *t* and *l* based on S_i and S_{Ti} for exchanger volume.

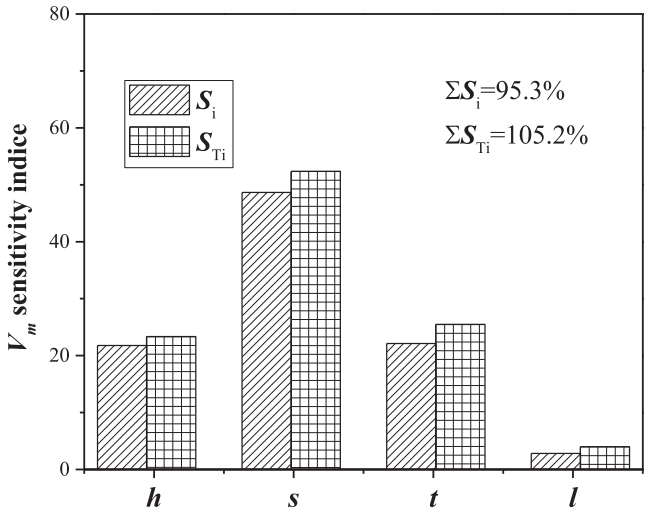

Fig. 5. Evolution of effect of parameters of *h*, *s*, *t* and *l* based on S_i and S_{Ti} for exchanger material content.

4.1.2. Fixed heat flow rate and pressure drop

As described in Section 2.1, when the mass flow rate, heat flow rate and pressure drop are fixed, the variation of fin height *h*, fin space *s*, fin thickness *t* and interrupted length *l* can cause the minor variation of the aspect rate *j*/*f* and fin efficiency η_o that results in the change of *Re*. So the above study, the changing *Re* will affect the values of the Sobol sensitivity indices of fin height *h*, fin space *s*, fin thickness *t* and interrupted length *l*. To solve this problem, the effects of *Re*, fin height *h*, fin space *s*, fin thickness *t* and interrupted length *l* on heat exchanger volume and material content are studied under given heat flow rate and pressure drop.

The Sobol sensitivity indices of *Re*, fin height *h*, fin space *s*, fin thickness *t* and interrupted length *l* on heat exchanger volume and material content are presented in Figs. 6 and 7 under given heat flow rate and pressure drop. As shown, the effects of *Re* and fin space *s* on the exchanger volume and material content are high, while the effects of fin thickness *t* and interrupted length *l* are very

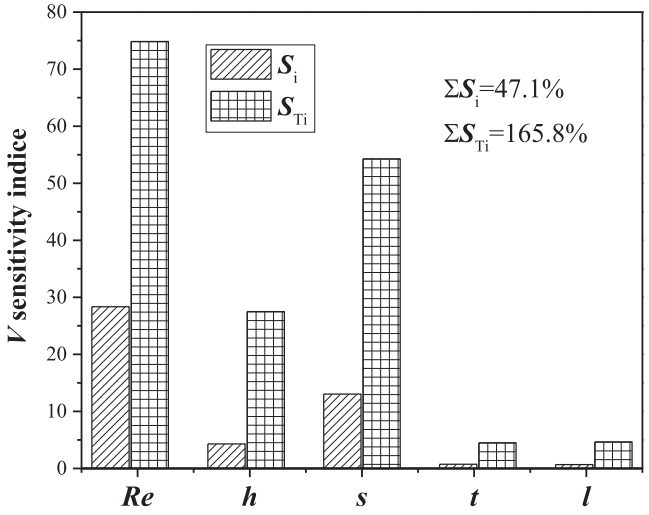

Fig. 6. Evaluation of effects of different parameters on exchanger volume.

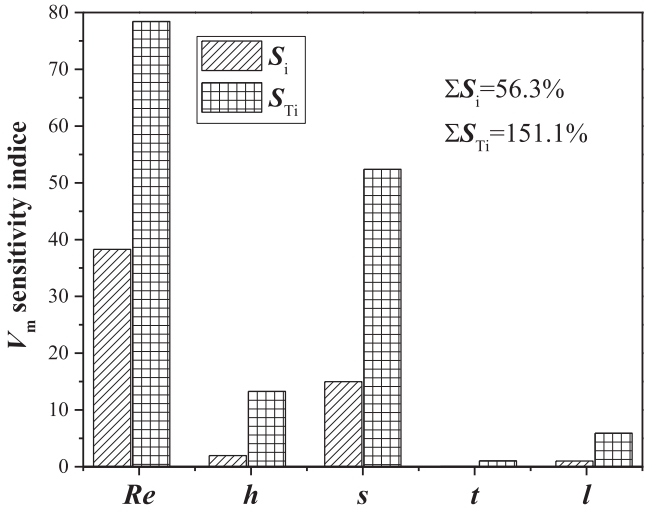

Fig. 7. Evaluation of effects of different parameters on exchanger material content.

Table 2
Main and high-order interaction effects of parameters on exchanger volume and material content.

Variables	Volume V	Material content V_m
Re	28.35	38.28
h	4.30	1.97
s	13.04	14.99
t	0.74	0.05
l	0.67	1.01
Re·h	7.98	3.69
Re·s	24.21	27.90
Re·h·s	12.98	6.58
Other	7.74	0.67

low. The sums of first order sensitivity indices and total-order sensitivity indices of parameters on the heat exchanger volume are 47.1% and 165.8%, respectively. And those of parameters on the heat exchanger material content are 56.3% and 151.1%, respectively. Therefore, it can be obtained, when the heat flow rate and pressure drop are fixed, the effects of interactions among *Re*, fin height *h*, fin space *s*, fin thickness *t* and interrupted length *l* on the exchanger volume and exchanger material are significant. A paradoxical conclusion with the above results can be explained in Table 2. As shown, the high-order interaction effects among

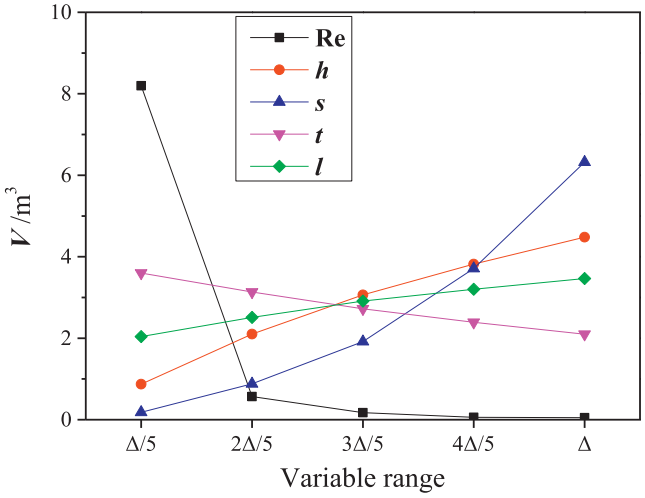

Fig. 8. Mean value of exchanger volume versus variable range.

Re, fin height *h* fin space *s* are apparent, while the other high-order interaction effects can be ignored since their sums are 7.7% and 5.5% on heat exchanger volume and material content, respectively. Therefore, it can be inferred that when the heat flow rate and pressure drop are fixed, the effects of fin height *h*, fin space *s*, fin thickness *t* and interrupted length *l* on heat exchanger volume and material content are mutually independent, while the interaction effects among *Re*, fin height *h* and fin space *s* are apparent, especially the second-order interaction effects between *Re* and fin space *s*.

In order to reveal the variation trend of heat exchanger volume and material content with the parameters, the average values of heat exchanger volume and material content are computed in the case of fixing one parameter and changing the other parameters. It is defined as: $I_i = E(Y|X_i)$. These results are shown in Figs. 8 and 9, in which the values of Δ is equal to the range of the parameters. As shown, the effects of *Re* on the heat exchanger volume and material content show negative growth and those of fin height *h*, fin space *s* and interrupted length *l* show positive growth. Moreover, the effect of the fin thickness *t* on heat exchanger volume shows negative growth, while its effect on material content shows positive growth. The average values of heat exchanger volume and material content decrease fast firstly and then decrease very slowly when the *Re* is from 200 to 2000. Therefore, to minimum the heat

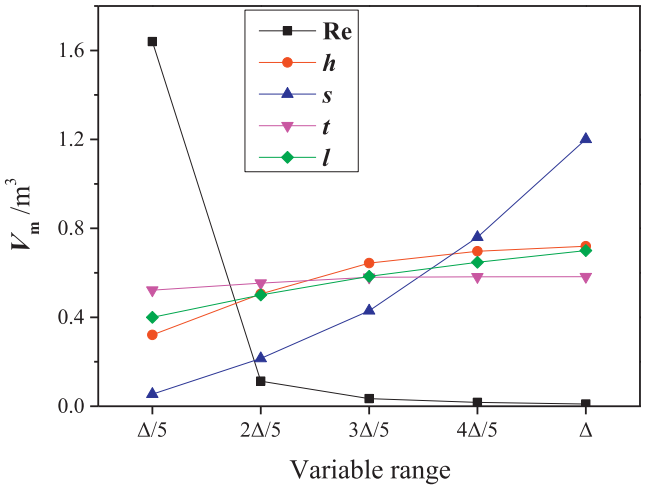

Fig. 9. Mean value of exchanger material content versus variable range.

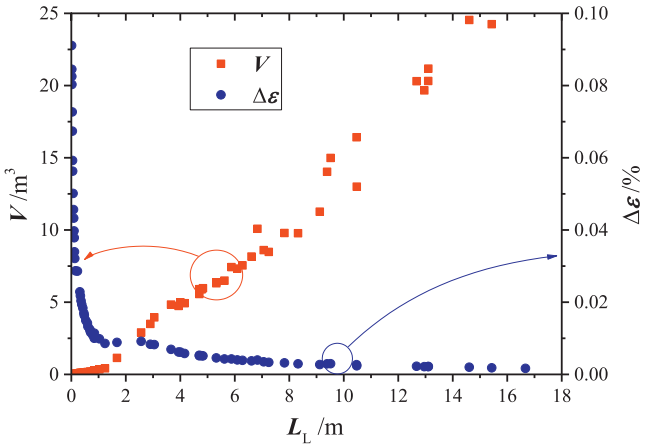

Fig. 10. Heat exchanger volume and effectiveness degradation rate due to longitudinal conduction versus flow length.

exchanger volume and material content with the heat flow rate and pressure drop limit, *Re* more than 650 is a selectable.

Fig. 10 shows the variation of heat exchanger volume and the effectiveness deterioration rate due to longitudinal conduction versus flow length. Clearly, the heat exchanger volume decreases as the flow length decreases. At the same time, the effectiveness deterioration rate due to longitudinal conduction increases rapidly as the flow length goes down to 1.0 m. Therefore, decreasing the heat exchanger volume implies the reduction of flow length. However, in this case, the longitudinal conduction due to the reduction in flow length should be taken into account, especially for cryogenic heat exchanger.

4.1.3. Fixed exchanger volume

The Sobol sensitivity indices of *Re*, fin height *h*, fin space *s*, fin thickness *t* and interrupted length *l* on heat flow rate and pressure drop are presented in Figs. 11 and 12 for fixed heat exchanger volume. The effect of *Re* on the heat flow rate is the highest, that of fin space *s* is second, while those of fin height *h*, fin thickness *t* and interrupted length *l* are very low (Fig. 11). As shown in Fig. 12, the interaction effects of *Re*, fin space *s*, fin thickness *t* and interrupted length *l* on pressure drop are all not ignorable, in which the sums of first order sensitivity indices and total-order sensitivity indices of parameters are 46% and 171.8%, respectively.

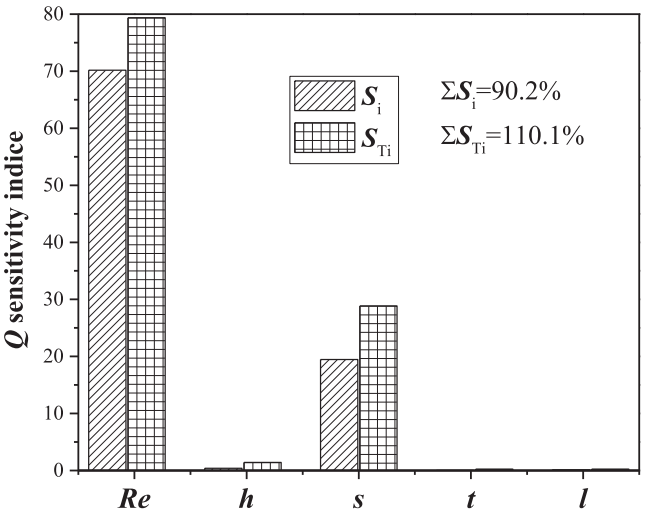

Fig. 11. Evaluation of effects of different parameters on heat flow rate.

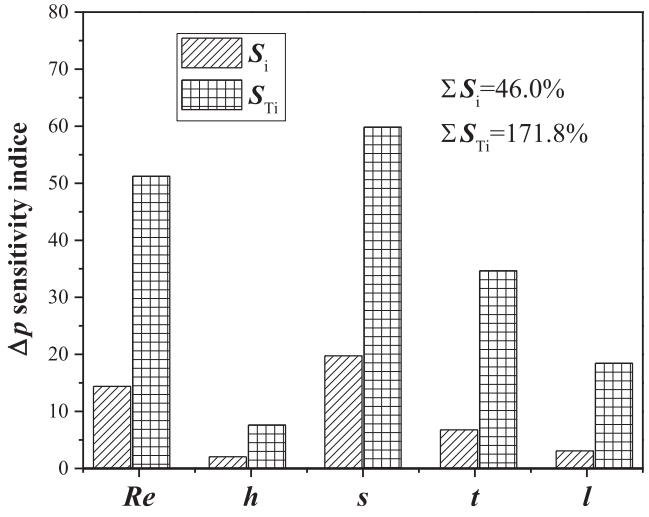

Fig. 12. Evaluation of effects of different parameters on pressure drop.

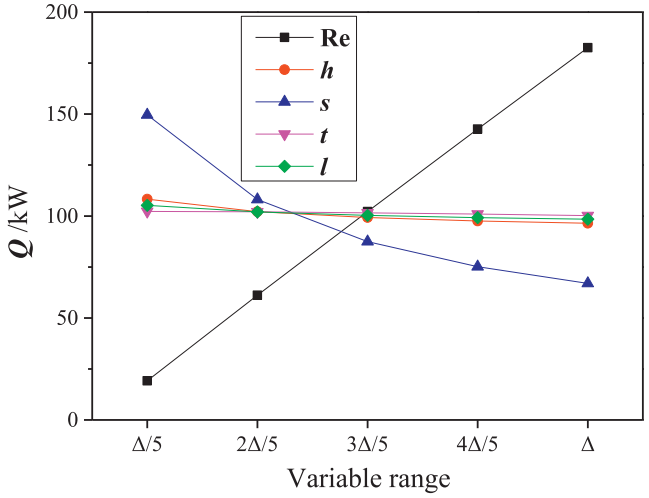

Fig. 13. Mean value of heat flow rate for different parameters.

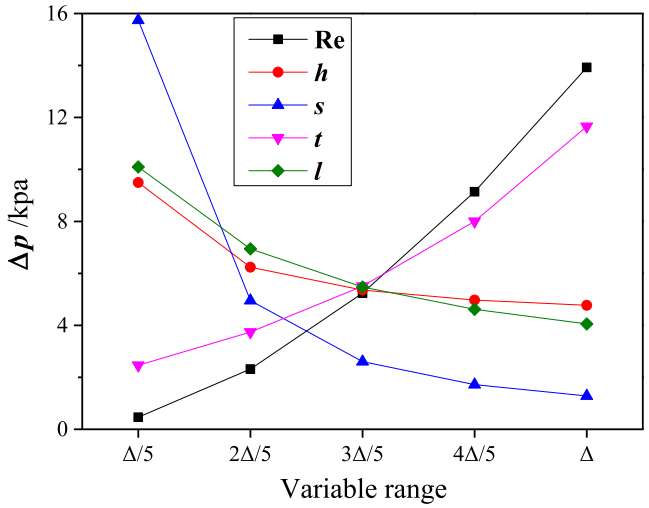

Fig. 14. Mean value of pressure drop for different parameters.

The mean values of heat flow rate and pressure drop versus *Re*, fin height *h*, fin space *s*, fin thickness *t* and interrupted length *l* are shown in Figs. 13 and 14 respectively under fixed heat exchanger volume. It can be observed that the effects of Re on heat flow rate and pressure drop show positive growth and those of fin height *h*,

fin space s and interrupted length l show negative growth. The effect of the fin thickness t on heat flow rate shows negative growth, while it on pressure drop shows positive growth. Therefore, a smaller fin thickness is beneficial to enhance heat flow rate and decrease pressure drop. Besides, considering the effects of fin height h and interrupted length l on heat flow rate are very low, they can be designed a larger value to decrease the pressure drop of heat exchanger.

4.2. Compared with the effect of parameters according to Prandtl number

In Figs. 15 and 16, the Sobol sensitivity indices of parameters on heat flow rate and pressure drop are compared under given the heat exchanger volume. The Prandtl number for air and water are 0.744 and 6.99, respectively. As shown in Fig. 15, the effects of parameters on heat flow rate are similar. The high-order interaction effects among these parameters on heat flow rate can be ignored except the second-order interaction effects between *Re* and other parameters. In Fig. 16, the effects of parameters on pressure drop show significant differences for air and water. Besides, the high-order interaction effects among these parameters are also high, especially the interaction effects among *Re*, fin space *s* and fin thickness *t*.

In Figs. 17 and 18, the total-order sensitivity indices of *Re*, fin height *h*, fin space *s*, fin thickness *t* and interrupted length *l* on heat

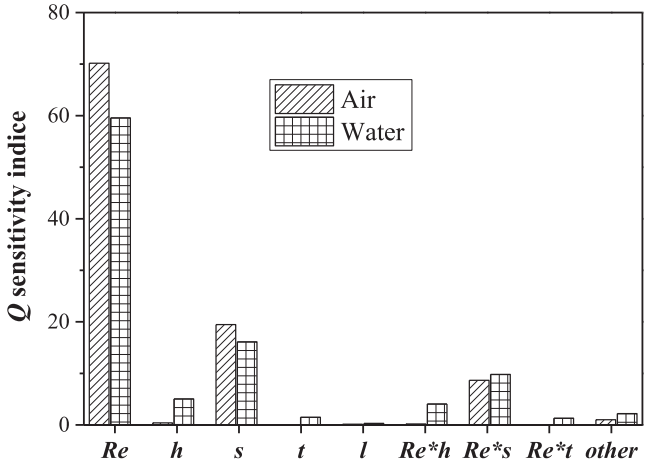

Fig. 15. The effect of parameters on heat flow rate for different medium.

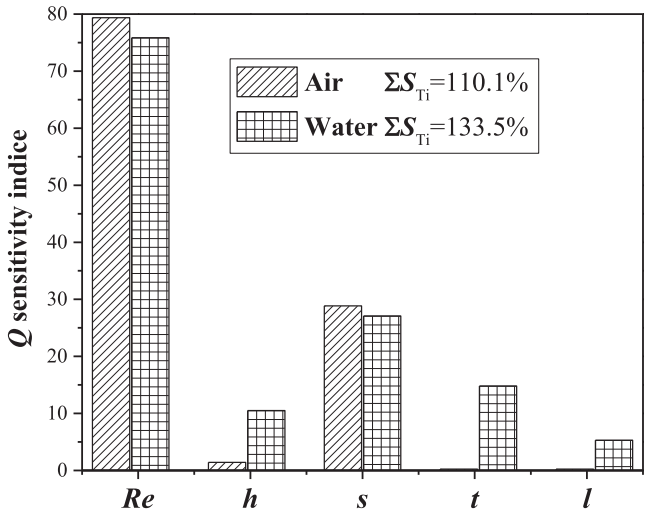

Fig. 17. Total-order sensitivity indices of parameters on heat flow rate for different medium.

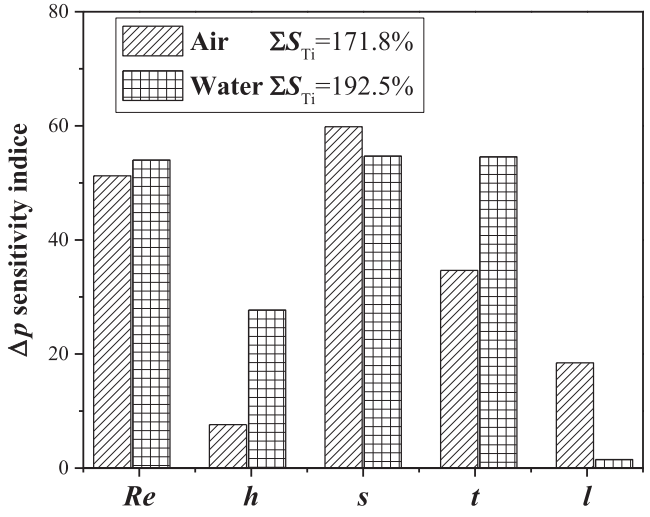

Fig. 18. Total-order sensitivity indices of parameters on pressure drop for different medium.

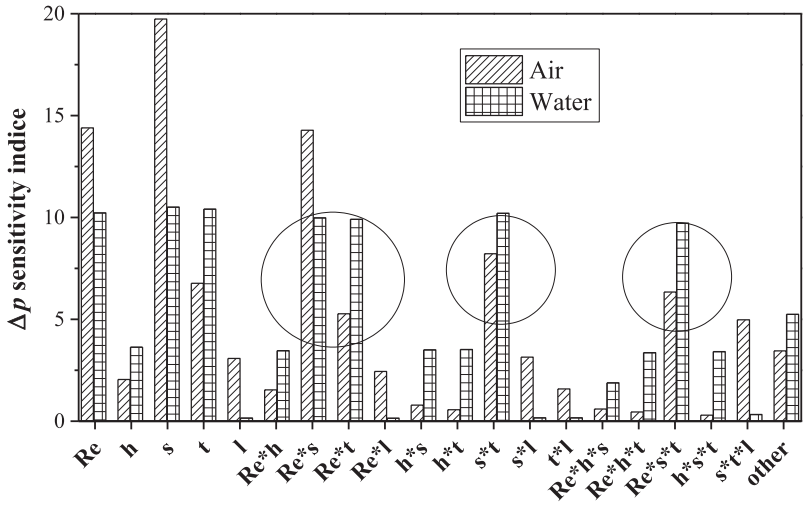

Fig. 16. The effect of parameters on pressure drop for different medium.

flow rate and pressure drop are shown under given the exchanger volume. The effects of *Re* and fin space *s* of water on heat flow rate and pressure drop are very close to those of air, while the effects of fin height *h* and fin thickness *t* on heat flow rate and pressure drop are higher for water. Besides, compared with air, the effect of interrupted length *l* on heat flow rate for water is higher and is lower on pressure drop. Therefore, compared with air, the interrupted length *l* for water should be selected a smaller value to enhance the heat flow rate with a small pressure drop penalty. Moreover, based on the variation trend of heat flow rate and pressure drop versus the different parameters, it can be inferred that compared with air, the fin height *h* should be chosen a smaller value and the fin thickness *t* should be designed a bigger value for water.

5. Conclusions

In this paper, Sobol sensitivity analysis was applied to evaluate quantitatively the effects of input parameters on the performance of PFHE with serrated fin. The main conclusions are as follows:

(1) The Sobol sensitivity study can quantify the effects of parameters that enable help designer to better select the suitable fin surface during the design procedure of PFHE. Compared with other optimization algorithms, this method is simple to implement.
(2) As the heat flow rate and pressure drop limited, the effects of *Re* and fin space *s* on the heat exchanger volume and material content are very important, in which the effect of *Re* on objective functions shows negative growth, while that of fin space shows positive growth. Besides, the high-order interaction effects among *Re*, fin height *h* fin space *s* are obvious.
(3) As the heat exchanger size limited, the effects of *Re* and fin space *s* heat flow rate and pressure drop are very important, in which the effect of *Re* on objective functions shows positive growth, while that of fin space shows negative growth. The interaction effects of input parameters on heat flow rate are low. However, those of input parameters on pressure drop are significant.
(4) As the heat exchanger size limited, the effect of the fin thickness *t* on heat flow rate shows negative growth and it shows positive growth on pressure drop. Therefore, a smaller fin thickness *t* is beneficial to enhance heat flow rate and decrease pressure drop.
(5) As the heat exchanger size limited, compared with air, the effect of interrupted length *l* on heat flow rate is higher and is lower on pressure drop for water. However, the effects of interrupted length *l* on heat flow rate and pressure drop show negative growth. Therefore, compared with air, the interrupted length *l* should be selected a smaller value for water.

Acknowledgements

This work was supported by the National Natural Science Foundation of China (51676146), Key Laboratory of Advanced Reactor Engineering and Safety, Ministry of Education, Tsinghua University, for which the authors are thankful.

Conflict of interest

We declare that we do not have any commercial or associative interest that represents a conflict of interest in connection with the work submitted.

Appendix A. Supplementary materials

Supplementary data associated with this article can be found, in the online version, at http://dx.doi.org/10.1016/j.ijheatmasstransfer.2017.08.089.

References

[1] J.E. Hesselgreaves, Compact Heat Exchangers: Selection, Designed and Operation, Elsevier Science Ltd., UK, 2001.
[2] Yuanyuan Zhou, Lin Zhu, Yu. Jianlin, Yanzhong Li, Optimization of plate-fin heat exchangers by minimizing specific entropy generation rate, Int. J. Heat Mass Transf. 78 (2014) 942–946.
[3] H. Najafia, B. Najafi, P. Hoseinpoori, Energy and cost optimization of a plate and fin heat exchanger using genetic algorithm, Appl. Therm. Eng. 31 (2011) 1839–1847.
[4] J. Wen, H.Z. Yang, G.P. Jian, X. Tong, K. Li, S.M. Wang, Energy and cost optimization of shell and tube heat exchanger with helical baffles using Kriging metamodel based on MOGA, Int. J. Heat Mass Transf. 98 (2016) 29–39.
[5] S. Sanaye, H. Hajabdollahi, Thermal-economic multi-objective optimization of plate fin heat exchanger using genetic algorithm, Appl. Energy 87 (2010) 1893–1902.
[6] J. Wen, H.Z. Yang, X. Tong, K. Li, S.M. Wang, Y.Z. Li, Optimization investigation on configuration parameters of serrated fin in plate-fin heat exchanger using genetic algorithm, Int. J. Therm. Sci. 101 (2016) 116–125.
[7] M. Yousefi, A.N. Darus, H. Mohammadi, An imperialist competitive algorithm for optimal design of plate-fin heat exchangers, Int. J. Heat Mass Transf. 55 (2012) 3178–3185.
[8] H. Peng, X. Ling, E. Wu, An improved particle swarm algorithm for optimal design of plate-fin heat exchangers, Ind. Eng. Chem. Res. 49 (2010) 6144–6149.
[9] R.V. Rao, V.K. Patel, Thermodynamic optimization of cross flow plate-fin heat exchanger using a particle swarm optimization algorithm, Int. J. Therm. Sci. 49 (2010) 1712–1721.
[10] M. Yousefi, M. Yousefi, R.P.M. Ferreira, A.N. Darus, A swarm intelligent approach for multi-objective optimization of compact heat exchangers, Part E: J. Process Mech. Eng. 231 (2017) 164–171.
[11] H. Peng, X. Ling, Optimal design approach for the plate-fin heat exchangers using neural networks cooperated with genetic algorithms, Appl. Therm. Eng. 28 (2008) 642–650.
[12] M. Yousefi, R. Enayatifar, A.N. Darus, Optimal design of plate-fin heat exchangers by a hybrid evolutionary algorithm, Int. Commun. Heat Mass Transfer 39 (2012) 258–263.
[13] M. Yousefi, A.N. Darus, M. Yousefi, D. Hooshyar, Multi-stage thermal-economical optimization of compact heat exchangers: a new evolutionary-based design approach for real-world problems, Appl. Therm. Eng. 83 (2015) 71–80.
[14] W.M. Kays, A.L. London, Compact Heat Exchanger, second ed., McGraw. Hill, New York, 1964.
[15] S.V. Manson, Correlations of Heat Transfer Data and of Friction Data for Interrupted Plane Fins Staggered in Successive Rows, NACA Tech. Note 2237, National Advisory Committee for Aeronautics, Washington, DC, December 1950.
[16] R.L. Webb, H.M. Joshi, A friction factor correlation for the offset fin matrix, Heat Trans. Hemisphere Washington, DC 6 (1982) 257–262.
[17] A.R. Wieting, Empirical correlations for heat transfer and flow friction characteristics of rectangular offset-fin plate-fin heat exchangers, Heat Transfer 30 (1975) 69–84.
[18] S. Mochizuki, Y. Yagi, W.J. Yang, Transport phenomena in stacks of interrupted parallel-plate surfaces, Exp. Heat Transfer 1 (1987) 127–140.
[19] E.V. Dubrovsky, V.Y. Vasiliev, Enhancement of convective heat transfer in rectangular ducts of interrupted surfaces, Int. J. Heat Mass Transfer 31 (1988) 807–818.
[20] R.M. Manglik, A.E. Bergles, Heat transfer and pressure drop correlations for the rectangular offset strip fin compact heat exchanger, Exp. Therm. Fluid Sci. 10 (1995) 171–180.
[21] Y.J. Yang, Y.Z. Li, General prediction of the thermal hydraulic performance for plate-fin heat exchanger with offset strip fins, Int. J. Heat Mass Transf. 78 (2014) 860–870.
[22] M.S. Kim, J. Lee, S.J. Yook, K.S. Lee, Correlations and optimization of a heat exchanger with offset-strip fins, Int. J. Heat Mass Transf. 54 (2011) 2073–2079.
[23] S. Hu, K.E. Herold, Prandtl number effect on offset fin heat exchanger performance: experimental results, Int. J. Heat Mass Transf. 38 (1995) 1053–1061.
[24] W. Tian, A review of sensitivity analysis methods in building energy analysis, Renew. Sustain. Energy Rev. 20 (2013) 411–419.
[25] P.P.P.M. Lerou, T.T. Veenstra, J.F. Burger, H.J.M. Brake, H. Rogalla, Optimization of counterflow heat exchanger geometry through minimization of entropy generation, Cryogenics 45 (2005) 659–669.
[26] J. Wen, H.Z. Yang, X. Tong, K. Li, S.M. Wang, Y.Z. Li, Configuration parameters design and optimization for plate-fin heat exchangers with serrated fin by multi-objective genetic algorithm, Energy Convers. Manage. 117 (2016) 482–489.

[27] I. Kotcioglu, A. Cansiz, M.N. Khalaji, Experimental investigation for optimization of design parameters in a rectangular duct with plate-fins heat exchanger by Taguchi method, Appl. Therm. Eng. 50 (2013) 604–613.
[28] M. Fesanghary, E. Damangir, I. Soleimani, Design optimization of shell and tube heat exchangers using global sensitivity analysis and harmony search algorithm, Appl. Therm. Eng. 29 (2009) 1026–1031.
[29] Z.G. Qi, J.P. Chen, Z.J. Chen, Parametric study on the performance of a heat exchanger with corrugated louvered fins, Appl. Therm. Eng. 27 (2007) 539–544.
[30] F.R. Menter, Two-equation eddy-viscosity turbulence models for engineering applications, AIAA J. 32 (8) (1994) 1598–1605.